

## Observation of the Transverse Optical Plasmon in $\text{SmLa}_{0.8}\text{Sr}_{0.2}\text{CuO}_{4-\delta}$

Diana Dulić,<sup>1</sup> A. Pimenov,<sup>2</sup> D. van der Marel,<sup>1</sup> D. M. Broun,<sup>3,4</sup> Saeid Kamal,<sup>3</sup> W. N. Hardy,<sup>3</sup> A. A. Tsvetkov,<sup>1</sup>  
I. M. Sutjaha,<sup>5</sup> Ruixing Liang,<sup>3</sup> A. A. Menovsky,<sup>5</sup> A. Loidl,<sup>2</sup> and S. S. Saxena<sup>1</sup>

<sup>1</sup>Laboratory of Solid State Physics, Materials Science Centre, Nijenborgh 4, 9747 AG Groningen, The Netherlands

<sup>2</sup>Experimentalphysik V, University of Augsburg, Universitaetsstrasse 2, 86135 Augsburg, Germany

<sup>3</sup>Department of Physics and Astronomy, University of British Columbia, Vancouver, British Columbia, V6T 1Z1, Canada

<sup>4</sup>Interdisciplinary Research Centre in Superconductivity and Department of Physics, Cavendish Laboratory, University of Cambridge, Madingley Road, Cambridge CB3 0HE, United Kingdom

<sup>5</sup>Van der Waals–Zeeman Instituut, University of Amsterdam, The Netherlands

(Received 25 October 2000)

We present microwave and infrared measurements on  $\text{SmLa}_{0.8}\text{Sr}_{0.2}\text{CuO}_{4-\delta}$ , which are direct evidence for the existence of a transverse optical plasma mode, observed as a peak in the  $c$ -axis optical conductivity. This mode appears as a consequence of the existence of two different intrinsic Josephson couplings between the  $\text{CuO}_2$  layers, one with a  $\text{Sm}_2\text{O}_2$  block layer, and the other one with a  $(\text{La}, \text{Sr})_2\text{O}_{2-\delta}$  block layer. From the frequencies and the intensities of the collective modes we determine the value of the compressibility of the two dimensional electron fluid in the copper oxygen planes.

DOI: 10.1103/PhysRevLett.86.4144

PACS numbers: 78.30.Er, 74.25.Gz, 74.72.Jt

In 1966 Leggett predicted for superconductors with two bands of charge carriers a collective oscillation corresponding to small fluctuations of the relative phases of the two condensates, briefly indicated as excitons below the superconducting gap [1]. In principle these excitons should be observable with electromagnetic radiation, but in practice the effect on the infrared optical properties of most superconducting materials has been too small to be observable, except for, as we will demonstrate in the present paper, the bilayer cuprate superconductors. The cuprate high temperature superconductors naturally form weakly coupled stacks of superconducting layers [2]. Some members of this family, e.g.,  $\text{Bi}_2\text{Sr}_2\text{CaCu}_2\text{O}_8$ , have two superconducting layers per unit cell. These materials are realizations of a two-band superconductor, satisfying the following unique conditions: (i) For polarization of the electric field perpendicular to the conducting planes the metallic screening is very weak due to strong anisotropy of the static and dynamical electrical conductivity. (ii) The dipole selection rules allow optical transitions which resonate at the Josephson exciton energy.

In Ref. [3] two of us (D. v. d. M. and A. A. T.) calculated the dielectric function for cuprate superconductors with two  $\text{CuO}_2$  planes per unit cell, using the Lawrence-Doniach model [2] with alternating coupling constants (the “multilayer model”). A direct consequence was the presence of a transverse optical plasma mode, polarized perpendicular to the planes for propagation along the planes. Similar to a transverse optical phonon, and in contrast to the transverse Josephson plasma resonance (JPR) in single layer cuprates, this mode is observable as an optically allowed absorption in measurements of the optical conductivity. In Fig. 1 the currents and charge oscillations of these modes are sketched. Recently the unusual “bump” in the  $c$ -axis conductivity of YBCO [4,5] and Bi2212 [6], has been attributed to such a mode. However, due to the close

proximity to the optical phonons it was not possible to separate these electronic collective modes from the optical lattice vibrations [5], which complicates the quantitative analysis of this interesting phenomenon.

Both in the two-band exciton model and in the multilayer model the collective modes are oscillations of the relative phase of the two condensates, the inertia of which is due to the finite Josephson coupling between the two condensates. In Ref. [1] the restoring force was provided by the fact, that if  $\delta N$  electrons are added to a plane, the free energy increases with an amount  $\delta F = \mu \delta N + \delta N^2 / (2Kn^2)$ . Here  $\mu$ ,  $K$ , and  $n$  are the chemical potential, the electronic compressibility, and the electron density, respectively. For a Fermi-liquid,  $Kn^2 = \partial N / \partial \mu$  corresponds to density of states at the Fermi level. In neutral fluids the compressibility causes propagation of sound, whereas for electrons it causes the dispersion of plasmons. On the other hand, in Ref. [3] the restoring force is

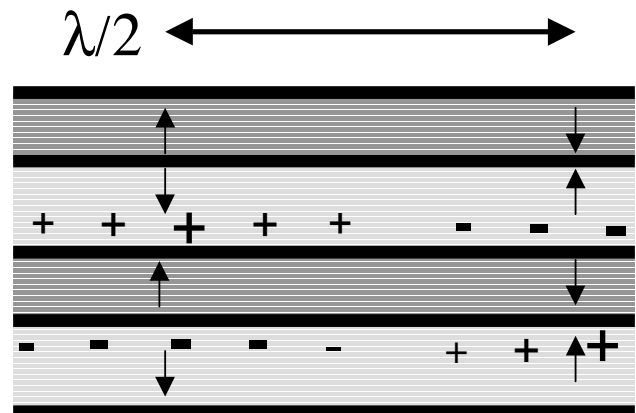


FIG. 1. Snapshot of the currents (arrows) and charges ( $\pm$  signs) of the transverse optical JPR. This mode carries a finite net polarization transverse to the direction of propagation.

provided by the long range Coulomb interaction between each set of planes. Recently, this model was extended by taking into account the compressibility [7]. Dispersion of the JPR in the cuprates due to the compressibility term has been previously described by Koyama and Tachiki [8].

$\text{SmLa}_{0.8}\text{Sr}_{0.2}\text{CuO}_{4-\delta}$  forms the  $T^*$  structure, with superconducting planes alternatingly separated by two types of blocking layers, a fluorite-type layer of  $\text{Sm}_2\text{O}_2$  ( $T'$  type) and a rocksalt-type  $(\text{La}, \text{Sr})_2\text{O}_{2-\delta}$  ( $T$  type) block layer. The lattice parameter is  $12.57 \text{ \AA}$ , and the distances between  $\text{CuO}_2$  layers across the  $\text{SmO}$  and the  $\text{LaO}$  barriers are  $6.13 \text{ \AA}$ , and  $6.43 \text{ \AA}$ , respectively [9]. Because the coupling across both blocking layers is weak, the Josephson plasma resonances are well below the optical phonon frequencies, allowing a clean separation between the lattice vibrations and the electronic modes. Recently *two* longitudinal Josephson plasma resonances have been observed [10] in embedded powder samples of this material using the far-infrared sphere resonance method, but the transverse optical plasma mode could not be detected.

In this Letter, we present infrared optical spectra of single crystal  $\text{SmLa}_{0.8}\text{Sr}_{0.2}\text{CuO}_{4-\delta}$ . We observed the transverse optical plasma mode and the two longitudinal Josephson plasma resonances. The influence of the compressibility on the intensity and the frequency of the observed resonances is large, a characteristic which these collective modes have in common with the two-band excitons predicted in 1966 [1]. Using a quantitative analysis of the intensities and peak positions of the three collective modes, we extract the values of the intrinsic Josephson coupling constants and the compressibility of the two dimensional charge fluid in the planes.

The single crystals of  $\text{SmLa}_{0.8}\text{Sr}_{0.2}\text{CuO}_{4-\delta}$  were grown at the University of Amsterdam using a four mirror image furnace. They were annealed at  $900 \text{ }^\circ\text{C}$  for 24 h to homogenize the strontium concentration. The crystal was cut into several slabs for the various experiments, and then annealed in a high pressure oxygen furnace at the University of British Columbia. The samples were slow cooled ( $1 \text{ }^\circ\text{C/h}$ ) from  $500$  to  $350 \text{ }^\circ\text{C}$  at 80 bars oxygen pressure, held at  $350 \text{ }^\circ\text{C}$  for 48 h and then quenched by opening the furnace. The large crystal faces (containing the  $c$  axis) were polished to an optical finish using diamond polishing pads. The magnetization, as measured in a field of 2 Oe with  $H$  parallel to  $c$ , gave a midpoint  $T_c$  of about 16 K with a transition width of  $\pm 2 \text{ K}$ .

Three types of experiments were performed: (a) polarized reflection measurements using a Fourier transform spectrometer in the frequency range between 12 and  $1000 \text{ cm}^{-1}$ , and the temperature range from 4 to 300 K; *in situ* evaporated gold films were used as a reference; (b) polarized transmission measurements in the frequency range from 4 to  $20 \text{ cm}^{-1}$  using a Mach-Zehnder interferometer arrangement [11], which allows measurements of both transmission and phase shift (from the Fresnel formulas, the absolute values of the complex dielectric function can be determined directly from the measurements); and

(c) microwave cavity perturbation measurements at 1, 25, and 39 GHz. For (a), the dimensions of the sample were  $0.7 \text{ mm} \times 5 \text{ mm} \times 6 \text{ mm}$  for the  $a$ ,  $b$ , and  $c$  directions, respectively. For (b), the  $a$  dimension was  $110 \text{ }\mu\text{m}$ , and for (c) the  $a$  dimensions were between 38 and  $56 \text{ }\mu\text{m}$ .

In Fig. 2 we show the  $c$ -axis reflectivity spectra of  $\text{SmLa}_{0.8}\text{Sr}_{0.2}\text{CuO}_{4-\delta}$  above and below  $T_c$ , in the frequency range from  $13$ – $700 \text{ cm}^{-1}$ . In the inset of Fig. 2 the frequency region from  $13$ – $50 \text{ cm}^{-1}$  has been shown in more detail. In this region the sample has become relatively transparent, and one can see interferences from the copper block at the back side of the sample. These Fabry-Perot interferences are absent from the mm-wave experiments, due to the fact that we used much thinner samples in that case. The important conclusion is that there is almost no temperature dependence of the spectra in the  $13$ – $700 \text{ cm}^{-1}$  frequency region. We measured transmission and phase shift data in the frequency region from  $4$ – $20 \text{ cm}^{-1}$ , for various temperatures. The corresponding optical properties are obtained directly by the use of the Fresnel formulas and the relation between the dielectric function and optical conductivity:  $\epsilon = 4\pi i\sigma/\omega$ . The real part of the optical conductivity, the real part of the dielectric function, and the loss function  $\text{Im}(-1/\epsilon)$  are shown in Figs. 3(a), 3(b), and 3(c), respectively.

In Ref. [3] the dielectric function has been derived for a material with two superconducting layers per unit cell. The crystal was treated as a stack of superconducting layers of infinitesimal thickness, with two different Josephson coupling constants  $J$  and  $K$ , distances between the neighboring planes  $x_I d$  and  $x_K d$ ,  $x_I + x_K = 1$ , and  $d$  is the lattice constant along the  $c$  direction. The total dielectric function was shown to be of the form

$$\frac{\epsilon_{av}^s}{\epsilon(\omega)} = \frac{\tilde{z}_I \omega^2}{\omega(\omega + i\gamma_I) - \omega_I^2} + \frac{\tilde{z}_K \omega^2}{\omega(\omega + i\gamma_K) - \omega_K^2}. \quad (1)$$

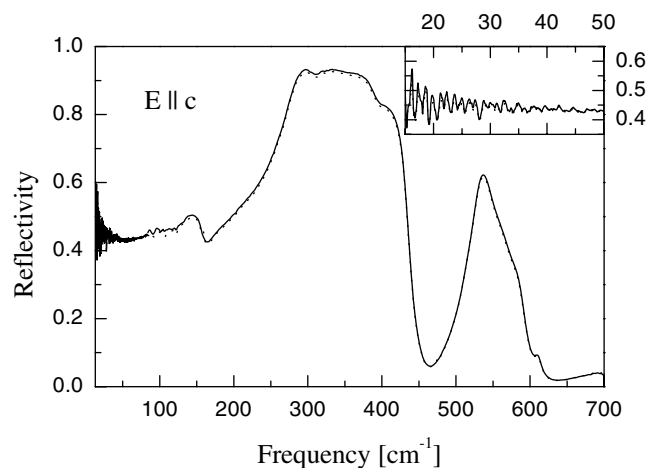


FIG. 2. The  $c$ -axis reflectivity of  $\text{SmLa}_{0.8}\text{Sr}_{0.2}\text{CuO}_{4-\delta}$ : 4 K—solid line; 30 K—dotted line. Inset: blown up region from 11 to  $50 \text{ cm}^{-1}$ .

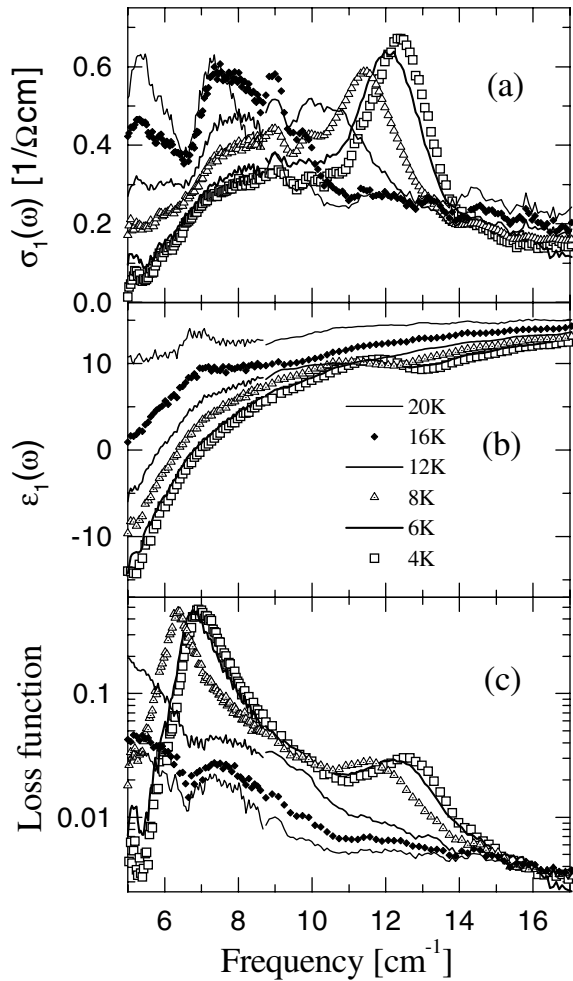


FIG. 3. (a) Real part of the  $c$ -axis optical conductivity for 4, 6, 8, 10, 16, and 20 K. (b) Real part of the  $c$ -axis dielectric function. The temperature labels corresponding to all three panels are indicated. (c) The  $c$ -axis loss function,  $\text{Im}\epsilon(\omega)^{-1}$ .

Here the average background dielectric constant is  $\epsilon_{\text{av}}^s = (x_I/\epsilon_I^s + x_K/\epsilon_K^s)^{-1}$ , and  $\epsilon_{\mu}^s$ ,  $\omega_{\mu}$ , and  $\gamma_{\mu}$  are the local background dielectric constants, the screened Josephson plasma frequencies, and the quasiparticle damping characterizing the two types of junctions.  $\text{Re}\epsilon(\omega)$  has two zero crossings corresponding to the two longitudinal plasmons, and a pole at the *transverse* optical plasma frequency. The transverse and the longitudinal plasma resonances show up as peaks in the optical conductivity and the loss function, respectively. The transverse optical plasma frequency  $\omega_T = (\tilde{z}_I\omega_K^2 + \tilde{z}_K\omega_I^2)^{1/2}$ , and its inverse lifetime  $\gamma_T = \tilde{z}_I\gamma_K + \tilde{z}_K\gamma_I$  are fixed by the values of  $\omega_I$ ,  $\omega_K$ ,  $\gamma_I$ ,  $\gamma_K$ , and the weight factors  $\tilde{z}_K = 1 - \tilde{z}_I$ , which are a function of the relative volume fractions, the local dielectric functions, and the compressibility which we will discuss below.

The two longitudinal plasma frequencies can be read directly from the peak positions in the loss function, providing  $\omega_I/2\pi c = 7 \text{ cm}^{-1}$  and  $\omega_K/2\pi c = 12.6 \text{ cm}^{-1}$ . The background dielectric constant is obtained by analyzing the reflectivity spectra of Fig. 2, providing

$\epsilon_{\text{av}}^s = 23.0 \pm 0.5$ . The intensities of the two peaks in the loss function or, more accurately, the intensity of the peak in  $\sigma$  at  $\omega_T$ , provide the weight factor  $\tilde{z}_K$ :  $\int \sigma_{\text{peak}}(\omega) d\omega = \tilde{z}_K \tilde{z}_I \epsilon_{\text{av}}^s (\omega_K^2 - \omega_I^2) / \omega_T^2$ . In this way we obtain  $\tilde{z}_K = 0.04 \pm 0.005$  and  $\tilde{z}_I = 0.96 \pm 0.005$ . In Fig. 4 we show the theoretical spectra of the conductivity, the real part of the dielectric function, and the loss function using these parameters together with the experimental spectra at 4 K. The damping factors were adjusted to the experimental linewidth of the loss peaks,  $\gamma_I/2\pi c = \gamma_K/2\pi c = 0.5 \text{ cm}^{-1}$ .

From the microwave data we have obtained an absolute measurement [12] of the  $c$ -axis penetration depth, which is  $45 \mu\text{m}$  at 3 K. The penetration depth is  $\lambda_c = \lim_{\omega \rightarrow 0} c / [\omega \text{Im}\sqrt{\epsilon(\omega)}]$ , which in the framework of Eq. (1) is  $\epsilon_{\text{av}}^s \lambda_c^2 / c^2 = \tilde{z}_I \omega_I^{-2} + \tilde{z}_K \omega_K^{-2}$ . With the experimental values for  $\tilde{z}_I$ ,  $\omega_I$ , and  $\omega_K$  determined above, this provides  $\lambda_c = 47 \mu\text{m}$ , in excellent agreement with the microwave results. In Fig. 5 the separate temperature dependencies of  $\lambda_c$ ,  $\lambda_{c,J}$ , and  $\lambda_{c,K}$  are given in the normalized

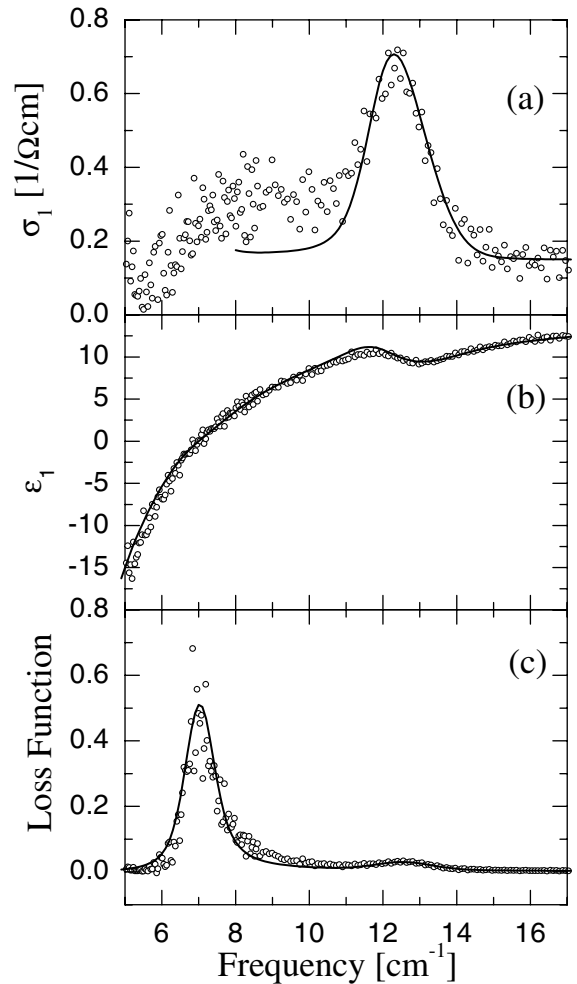


FIG. 4. (a) Fit (solid line) to (a) the real part of the  $c$ -axis optical conductivity, (b) Real part of the  $c$ -axis dielectric function, (c) the loss function at 3 K. The open circles are the experimental data.

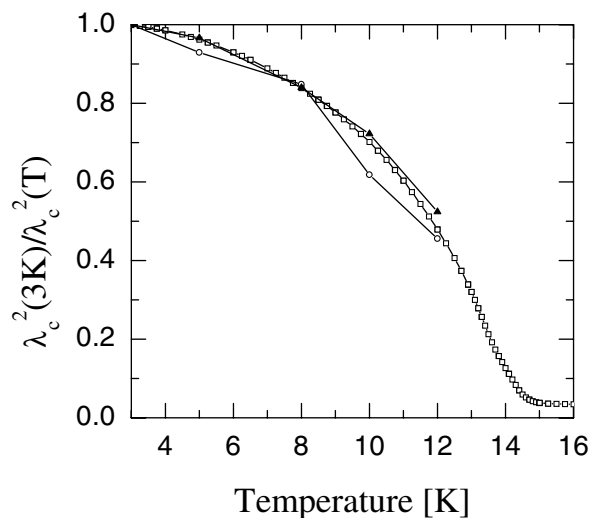


FIG. 5. Temperature dependence of the  $c$ -axis penetration depth: open squares—measured in cavity perturbation experiment; triangles:  $\lambda_{c,J}$ ; open circles:  $\lambda_{c,K}$ .

form  $\lambda_c^2(3K)/\lambda_c^2(T)$ ;  $\lambda_c$  is obtained from a 1 GHz cavity perturbation measurement, and  $\lambda_{c,J} = c/(\sqrt{\epsilon_I} \omega_I)$ ,  $\lambda_{c,K} = c/(\sqrt{\epsilon_K} \omega_K)$  from the transmission measurement. As seen from Fig. 5 both  $\lambda_{c,J}$  and  $\lambda_{c,K}$  exhibit similar, characteristic, power law temperature dependence  $\lambda_c^2(3K)/\lambda_c^2(T) = 1 - T^\eta$ ,  $\eta \sim 3$ . This establishes that both resonances are indeed Josephson plasmons.

The intensity of the peaks, represented by the weight factors,  $\tilde{z}_K = 0.04$  and  $\tilde{z}_I = 0.96$ , can be used to estimate the value of the compressibility of the 2D electron fluids, using the expressions derived in [7]. The dielectric function is of the form given in Eq. (1), while  $\tilde{z}_K$  can be calculated from the experimental peak positions and linewidths  $\omega_K$ ,  $\omega_I$ ,  $\gamma_I$ , and  $\gamma_K$  using

$$\tilde{z}_K = \frac{1}{2} + \frac{(z_K - z_I)(z_K z_I + 2\gamma)}{2(z_K z_I + 2\gamma + 4\gamma^2)} \times \sqrt{1 - \frac{4(2\gamma)^2 \omega_K^2 \omega_I^2}{(z_K z_I + 2\gamma)(\omega_K^2 - \omega_I^2)^2}} - \frac{2\gamma(z_K z_I + \gamma)}{z_K z_I + 2\gamma + 4\gamma^2} \frac{\omega_K^2 + \omega_I^2}{\omega_K^2 - \omega_I^2}. \quad (2)$$

Here  $\gamma$  is a dimensionless constant which is inversely proportional to the two-dimensional compressibility of the electron fluids in the planes,  $\gamma = \epsilon_{av}^s/(4\pi d e^2 K n^2)$ . The constants  $z_K$  and  $z_I$ , defined as  $z_K = x_K \epsilon_{av}^s/\epsilon_K^s$  and  $z_I = \epsilon_{av}^s/\epsilon_I^s$ , correspond to the weight factors in the limit of infinite compressibility ( $\gamma \rightarrow 0$ ). We can calculate them easily from the known volume fractions  $x_K$  and  $x_I$  (0.5 in the present case), and from the ratio between the  $T$ -phase and the  $T'$ -phase  $c$ -axis dielectric constants  $\epsilon_K^s/\epsilon_I^s$ . From infrared spectra of  $T$ -phase and the  $T'$ -phase materials [13], this ratio is known to be in the interval  $1 \leq \epsilon_K^s/\epsilon_I^s \leq 1.7$  [13]. The (numerical) inversion of Eq. (2) then provides  $Kn^2 = 1.12 \pm 0.01$  eV<sup>-1</sup> per unit of CuO<sub>2</sub>. For

La<sub>2-x</sub>Sr<sub>x</sub>CuO<sub>4-δ</sub> the linear term in the normal state specific heat [14] ranges from 0.4 mJ/g atom K<sup>2</sup> ( $x = 0.1$ ) to 1.2 mJ/g atom K<sup>2</sup> ( $x = 0.2$ ). For fermionic excitations this would imply that the density of states varies from 1.2 eV<sup>-1</sup> ( $x = 0.1$ ) to 5.0 eV<sup>-1</sup> per unit of CuO<sub>2</sub> ( $x = 0.2$ ). The value of  $Kn^2 = 1.1$  eV<sup>-1</sup> should then be taken as an indication, that our SmLaSrCuO crystals are underdoped. This is also indicated by the  $T_c$  of 16 K, and the low values of the JPR frequencies.

Without the compressibility term, the JPR's would have been at 6.1 and 8.0 cm<sup>-1</sup> [7]. Hence the finite electronic compressibility causes a large shift of resonance frequency and a large reduction of the intensity of the higher frequency JPR. This also explains why the “bump” has a very weak intensity in Bi2212 [6].

In conclusion, we have studied microwave and infrared properties of SmLa<sub>0.8</sub>Sr<sub>0.2</sub>CuO<sub>4-δ</sub>. We have observed two longitudinal Josephson plasma resonances, and the transverse optical plasma mode that arises from the alternation of two different Josephson couplings between the CuO<sub>2</sub> layers. We observe a shift of frequency of the plasma modes, and a reduction in intensity of the highest mode due to the finite electronic compressibility corresponding to 1.1 eV<sup>-1</sup> per CuO<sub>2</sub> unit.

We gratefully acknowledge Lev N. Bulaevskii for pointing out the importance of dispersion effects for the optical spectra. One of us (D.M.B.) wants to thank the Peter House College for financial support. This investigation was supported by the Netherlands Foundation for Fundamental Research on Matter (FOM) with financial aid from the Nederlandse Organisatie voor Wetenschappelijk Onderzoek (NWO).

- [1] A. J. Leggett, *Prog. Theor. Phys.* **36**, 901 (1966).
- [2] W. E. Lawrence and S. Doniach, in *Proceedings of the 12th International Conference on Low Temperature Physics, Kyoto, 1970*, edited by E. Kanda (Keigaku, Tokyo, 1970).
- [3] D. van der Marel and A. A. Tsvetkov, in *Proceedings of the 21st International Conference on Low Temperature Physics, Prague, 1996*, edited by S. Danis, V. Gregor, and K. Zaveta (Academy of Sciences of the Czech Republic, Praha, 1996); *Czech. J. Phys.* **46**, 3165 (1996).
- [4] M. Grüninger *et al.*, *Phys. Rev. Lett.* **84**, 1575 (2000).
- [5] D. Munzar *et al.*, *Solid State Commun.* **112**, 365 (1999).
- [6] V. Zelezny *et al.*, *J. Low Temp. Phys.* **117**, 1019–1024 (1999).
- [7] D. van der Marel and A. A. Tsvetkov (to be published); <http://xxx.lanl.gov/abs/cond-mat/0102303>
- [8] T. Koyama and M. Tachiki, *Phys. Rev. B* **54**, 16 183 (1996).
- [9] Y. Tokura *et al.*, *Phys. Rev. B* **40**, 2568 (1989).
- [10] H. Shibata and T. Yamada, *Phys. Rev. Lett.* **81**, 3519 (1998).
- [11] A. A. Volkov *et al.*, *Infrared Phys.* **25**, 365 (1985).
- [12] D. Broun and S. Kamal (unpublished).
- [13] S. Tajima *et al.*, *Phys. Rev. B* **43**, 10 496 (1991).
- [14] J. W. Loram *et al.*, *Physica (Amsterdam)* **235C–240C**, 134 (1994).